Fluid-induced anthropogenic and natural earthquake swarms driven by aseismic slip

Philippe Danré [1*], Louis De Barros [1], Frédéric Cappa [1,2], Jean-Paul Ampuero[1]

[1] Université Côte d'Azur, CNRS, Observatoire de la Côte d'Azur, IRD, Géoazur, France

[2] Institut Universitaire de France, Paris

Corresponding author: Philippe Danré (danre@geoazur.unice.fr)

Key Points:

- Scaling laws show that injection-induced and natural earthquake swarms have the same driving mechanism.
- We show that aseismic slip is always present in swarms, although its contribution differs from one swarm to another.
- We propose a model based on fluid-induced aseismic slip propagation that explains swarms behavior.

Abstract

Anthropogenic fluid injections at depth induce seismicity which is generally organized as swarms, clustered in time and space, with moderate magnitudes. While some similarities between swarms have already been observed, whether they are driven by the same mechanism is still an open question. Pore fluid pressure or aseismic processes are often proposed to explain observations, while recent models suggest that seismicity is triggered by fluid-induced aseismic slip. Using 22 natural and anthropogenic swarms, we observe that duration, migration velocity and total moment scale similarly for all swarms. This confirms a common driving process for natural and induced swarms and highlights the ubiquity of aseismic slip. We propose a method to estimate the seismic-to-total moment ratio, which is then compared to a theoretical estimation that depends on the migration velocity, the effective stress drop and the slip velocity. Our findings lead to a generic explanation of swarms driving process.

Plain Language Summary

Swarms are a particular type of seismic sequence, during which many earthquakes occur but with no mainshock distinguishable from the other events. They can be induced by anthropic injections at depth, like during geothermal exploitation. Natural swarms are also observed in a large variety of geological contexts. Natural and injection-induced swarms share a lot of similarities, like the migration of seismicity. But little is still known about their physics. Here, we explain the observed similarities by the fact that both types of swarms correspond to earthquakes triggered by the propagation of an aseismic slip transient, induced by fluid circulation. This allows to reconcile observations made over different length- and timescales, and provides a generic explanation of the processes occurring at depth.

1. Introduction

1.1 Natural and injection-induced swarms exhibit many similarities

Fluid pressure changes at depth can induce seismicity, as shown by the increase in seismicity near fluid injection sites during geothermal activities (e.g., in Basel, Switzerland; Diechmann and Giardini, 2009), wastewater storage in Oklahoma (Hincks et al., 2018), or during fault activation experiments in France (Guglielmi et al., 2015). On the other hand, earthquake swarms of natural origin (i.e., sequences of clustered earthquakes with moderate magnitudes, generally below $M_w = 5$, without a mainshock-aftershock pattern) occur in various geological and tectonic contexts, such as mountain ranges (Jenatton et al., 2007), rift zones (De Barros et al., 2020) or along transform faults (Roland and McGuire, 2009). Earthquakes during those swarms are located over one or several fault planes *(*Lohman et McGuire, 2007; Baisch et al., 2009: Hong et al., 2020; Fischer et Hainzl, 2021*).* Migration of seismicity is the most characteristic behavior of both injection-induced and natural earthquake swarms (Goebel et Brodsky, 2018*;* Passarelli et al., 2018). Proposed physical explanations for swarm migration include fluid pressure diffusion (Shapiro et al., 1997), aseismic slip (Roland et McGuire, 2009), or a combination of both (De Barros et al., 2021), as well as cascading events (Fischer et Hainzl, 2021).

To gain deeper understanding into swarm processes and evaluate how generic they are, we compare injection-induced swarms with natural ones. Given the similarities identified between the two types of swarms, we aim at evaluating if a common mechanical process may drive swarms in different geological contexts and origins.

1.2 Understanding the role of aseismic slip in swarms

Aseismic moment release is thought to occur for injection-induced sequences, as revealed by moment-volume scaling relations (McGarr et Barbour, 2018*;* De Barros et al., 2019), by geodesy in the vicinity of a fluid injection site in the Brawley Basin (Wei et al., 2015), by measurements during field experiments (Guglielmi et al., 2015) or indirectly by studying repeating earthquakes during the Soultz-Sous-Forêt sequences (Bourouis and Bernard, 2007; Lengliné et al., 2014). The relatively weak values of seismic moment released compared to the spatial extent of seismicity also indicate that aseismic slip occurs over the whole seismicity area (Fischer and Hainzl, 2017). Aseismic slip has also been observed in association with natural swarms, using geodesy and slip inversions (Lohman and McGuire, 2007; Gualandi et al., 2017), or by studying dual velocity migrations and repeating earthquakes during the 2015 swarm in the Gulf of Corinth (De Barros et al., 2020). Nevertheless, geodetic observations of aseismic slip associated with swarms remain rare and difficult to achieve, given the depth, long duration and low deformation of such sequences.

Numerical modeling showed that the increase of the critical earthquake nucleation size with fluid pressure first leads to aseismic slip, which may outpace the diffusing pressure front (Bhattacharya and Viesca, 2019; Larochelle et al., 2021) and which triggers seismicity near its edges where shear stresses increase (Cappa et al., 2019; Wynants-Morel et al., 2020*)*.

As illustrated on Figure 1, and based on the previously mentioned observations, while aseismic slip is directly induced by fluid pressure, earthquake swarms seem to be triggered by the shear stress perturbation resulting from aseismic slip propagation over brittle asperities, rather than by fluid overpressure. In this case, seismicity migration would be related to the aseismic slip propagation, and not to the diffusion of fluids (Bhattacharya et al., 2019; De Barros et al., 2021).

This is analogous to the observed co-location of seismic and aseismic slip areas during large slow slip events (SSEs) in subduction zones, as in Cascadia (Bartlow et al., 2011). The seismic events (tremors or earthquakes) are triggered by the stress transfer from the SSEs, even though such SSEs are not necessarily driven by pore fluid pressure perturbation.

In this work, we aim at exploring the similairities between injection-induced sequences and natural swarms in a general way, in order to infer if both types of seismicity can be explained by a common process, and in which extent aseismic slip is driving them. Using a dataset of 22 seismic sequences, we first investigate scaling relations between moment, migration and duration and we compare them to slow-slip events observations. As aseismic slip seems to be a common feature among swarms, we then introduce a method to estimate the total and aseismic deformation. Finally, we propose a mechanical framework that relates the seismic to total ratio to seismic observables.

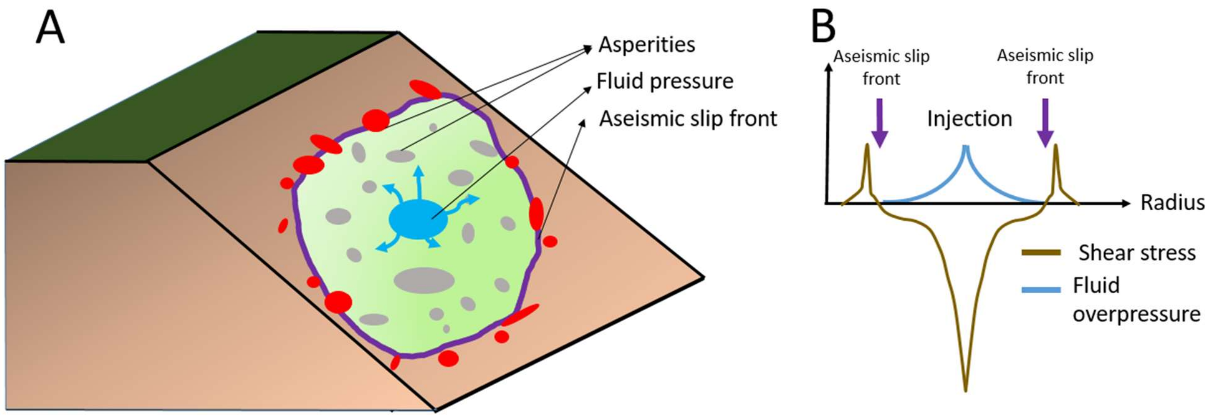

Figure 1. Common model for natural and induced swarms. (A) Conceptual view. Over a fault plane, fluid overpressure (blue arrows), either from anthropogenic or natural origin, induces aseismic slip (light green area). As the aseismic slip zone expands, it triggers seismicity near its edges (red patches) or within it (grey patches), through shear stress perturbation (brown curve, right). (B) Shear stress and fluid overpressure versus radial distance to the injection. The fluid overpressure induces an aseismic slip, with a shear stress drop within the slipping area and a stress concentration at its tip.

2. Materials and Methods

2.1 Data

We focus on a global dataset of 22 earthquake swarms, from either injection-induced or natural origin. For natural sequences, geological contexts are diverse: for instance, the 2003-2004 Ubaye swarm (Jenatton et al., 2007) occurs in a near-zero strain-rate area in the French Alps, while the 2015 Corinth swarm (De Barros et al., 2020) takes place in a very fast extensional (~15 mm/year) rift zone in Greece. We here focus on natural swarms in which fluid processes have been previously discussed, and we do not consider swarms taking place near volcanoes or in subduction zones. Most of the injection-induced swarms we consider originated from geothermal exploitation. However, they span a wide range of characteristics, including the injected fluid volume and the injection depth (see Supp.).

2.2 Migration velocity

Migration velocity of the 22 swarms is computed by fitting the seismicity front. Migration period is defined as the time during which the swarm is expanding. The spatial origin is chosen as the median of the coordinates of the 10 first events, and the origin time is defined as the time of the first event. We define the seismicity front as the 90th percentile of event distances in a sliding window containing 50 events. Seismicity front has been modelled by either diffusive law, linear fit or more complex relationships (Goebel et Brodsky, 2018; De Barros et al., 2021). The shape of the migration is here not investigated, as we only focus on an average migration velocity, in order to make comparisons among the different swarms. We fit a linear model over the seismicity front during the migration period of each sequence. This procedure yields migration durations and average migration velocities for each sequence (Figure 2A,B).

2.3 Seismicity area and effective stress drop computation

By analogy with the moment-size relationship for circular ruptures, the effective stress drop of a swarm is defined as (Fischer et Hainzl, 2017):

$$\boldsymbol{\Delta\sigma_e} = \frac{\boldsymbol{7M_{0,seismic}}}{\boldsymbol{16R^3}} \quad \text{(Equation 1)}$$

where R is the radius of the seismicity area and $\boldsymbol{M_{0,seismic}}$ the seismic moment released during the swarm. The effective stress drop value is an indicator of the relative importance of aseismic moment release (Fischer and Hainzl, 2017): a low effective stress drop suggests distant seismic asperities embedded in a fault slipping aseismically, while values close to earthquake static stress drops suggest that seismic asperities cover most of the slipping area.

Following Fischer and Hainzl (2017), seismicity area is computed by fitting a 2D plane over the 3D distribution of hypocenters, after removing the outsiders biasing the plane fitting. Hypocenters are then projected over the plane, and a ConvexHull algorithm delineates and returns the seismicity area S. We then compute a characteristic size, defined as $\boldsymbol{R = \sqrt{S/\pi}}$, and with the cumulative seismic moment value, we compute the effective stress drop.

2.4 Total moment estimation

Aseismic slip quantification is difficult for injection-induced sequences as deformations associated with those episodes are small (0.5mm for the Guglielmi et al., 2015 field experiment), over long durations, leading to small strain rates hard to observe. This issue stays the same for natural swarms.

We here propose a simple way to estimate, roughly, the aseismic slip. Studies of slow slip transients have shown that the slip released by repeating earthquake sequences equals the surrounding aseismic slip (Matsuzawa et al., 2004; Uchida, 2019). As the front of the swarm seismicity is assumed to be directly triggered by the shear stress perturbation induced by aseismic slip (Figure 1), we here make an analogy with slow slip transients. We suppose that the slip released seismically over discrete asperities equals the surrounding aseismic slip and neglect the afterslip (see Supp.). Assuming the asperity associated with the largest earthquake in the swarm only ruptures once, its slip gives an order of magnitude of the slip over the whole area. For each sequence, we isolate the largest event of moment $\boldsymbol{M_{0,max}}$ and assuming a circular rupture with a static stress drop $\boldsymbol{\Delta\sigma_{max}}$ of 10MPa (unless a more precise value is provided in the literature, see Supp.), we compute the slip $\boldsymbol{D_{max}}$ over this asperity (Madariaga, 1976) as:

$$\boldsymbol{D_{max} = M_{0,max}^{1/3} * \frac{(16\Delta\sigma_{max})^{2/3}}{G\pi 7^{2/3}}} \text{ (Equation 2)}$$

Given that seismic moment is released over brittle asperities and aseismic slip is released in between them, we estimate the total moment (seismic + aseismic) over the seismicity area as

$$\boldsymbol{M_{0,total} = G * D_{max} * S} \text{ (Equation 3)}$$

where G is the rock shear modulus (taken here as 30 GPa) and S the previously computed seismicity area. While the effective stress drop qualitatively indicates the importance of aseismic slip during a swarm, the rough quantification approach here allows us to better constrain aseismic moment release for each sequence.

2.5 Seismic to total moment ratio

By considering seismic and aseismic slip into one single slip event over a circular area of radius R, we have (Madariaga, 1976):

$$\boldsymbol{M_{0,total} = \frac{16}{7}\Delta\sigma_{total}R^3} \text{ (Equation 4)}$$

Where $\boldsymbol{\Delta\sigma_{total}}$ is the total stress drop over the studied area.

The rupture velocity of slow slip events is related to its stress drop and to its maximum slip velocity $\boldsymbol{V_{max}}$ (Ampuero and Rubin, 2008; Rubin, 2008; Passelègue et al., 2020) with:

$$\boldsymbol{V_{rupt}} = \frac{\boldsymbol{G*V_{max}}}{\boldsymbol{n*\Delta\sigma_{total}}} \text{ (Equation 5)}$$

To establish this, we assume that the stress drop of the slip event, $\boldsymbol{\Delta\sigma_{total}}$, is proportional (factor n > 1) to the associated strength drop. This can be observed in several numerical simulations of slow slip, where n~10 (Hawthorne and Rubin, 2013; Lambert et al., 2021).

In our case, we make the hypothesis that the seismicity is triggered by the fluid-induced aseismic slip. Therefore, the seismicity front follows the aseismic front (Wynants-Morel et al., 2020). The migration velocity of the swarms is then the rupture velocity of the aseismic slip ($V_{rupt} = V_{migr}$). Combining Equation 4 and Equation 5 we then have:

$$\boldsymbol{M_{0,total}} = \frac{\boldsymbol{16}}{\boldsymbol{7}} * \frac{\boldsymbol{G*V_{max}}}{\boldsymbol{n*V_{migr}}} * \boldsymbol{R^3} \text{ (Equation 6)}$$

This leads us to the following expression for the ratio *r* of seismic to total moment:

$$\boldsymbol{r} = \frac{\boldsymbol{M_{0,seismic}}}{\boldsymbol{M_{0,total}}} = \frac{\boldsymbol{7*M_{0,seismic}}}{\boldsymbol{16*R^3}} \frac{\boldsymbol{n*V_{migr}}}{\boldsymbol{G*V_{max}}} \text{ (Equation 7)}$$

This equation can be written in a more compact form using the effective stress drop (see Equation 1). We then get:

$$\boldsymbol{r} = \frac{\boldsymbol{n*\Delta\sigma_e*V_{migr}}}{\boldsymbol{G*V_{max}}} \text{ (Equation 8)}$$

This relation links the ratio of the cumulative seismic to total moment to the product of the migration velocity and the effective stress drop of the swarm.

3. Results

3.1 Aseismic slip drives the swarm's dynamics

The estimated velocities for the 22 swarms studied here range between a few meters per day, like for the Cahuilla swarm (Ross et al., 2020), to more than 1 km/day in the case of the Rittershoffen sequence (Lengliné et al., 2017). Figure 2C shows the migration velocity as a function of duration, for induced and natural swarms. For sake of comparison, we add the migration velocity of SSEs recorded on subduction zones (Gao et al., 2012). For these events, velocities correspond to the propagation of an aseismic slip, which is characterized either with geodesy (Schmidt and Gao, 2010) or with tremor migration (Bartlow et al., 2011; Ito et al., 2007).

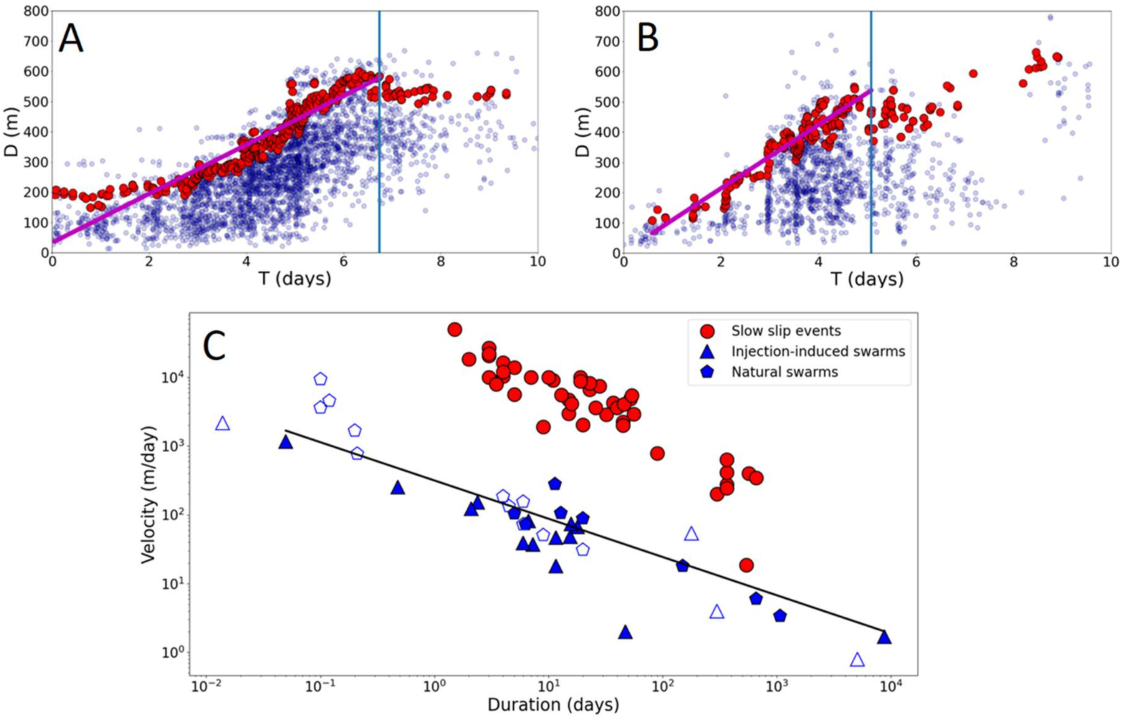

Figure 2. Scaling of propagation velocity with duration for swarms and slow slip events (SSEs). **(A)** Space-time distribution of seismicity in the Basel sequence (Herrmann et al., 2019*)*. Blue dots represent individual event hypocenters while red circles represent the computed seismicity front. Linear fitting (magenta line) over the seismicity migration period, delimited by the vertical blue line, yields a propagation velocity of 81 m/day. **(B)** Same but for the Corinth 2015 swarm (De Barros et al., 2020). The seismicity front migrates at a velocity of 105 m/day. **(C)** Scaling of

velocity with duration. Red dots represent SSE data from (Gao et al., 2012). Filled triangles and pentagons represent injection-induced and natural swarms, respectively, for which we determined migration velocity and duration based on seismicity catalogs. Empty symbols represent migration velocities and durations directly taken from the literature (see Supp.). Black line represents the best-fitting line between our computed velocities and durations ($R^2 = 0.76$).

Two main observations can be made. First, injection-induced and natural swarms follow the same scaling $\boldsymbol{V \alpha\, T^{-\gamma}}$ of velocity with duration, with $\boldsymbol{\gamma = 0.6}$ and $\boldsymbol{\gamma = 0.7}$ when considering each subset individually. In addition to the other similarities discussed beforehand, the continuous scaling of velocity with duration for all swarms is direct evidence that both types of sequences obey the same physics for all velocity ranges (from a few meters per day in Ubaye or Cahuilla to 1160 m/day for Rittershoffen). As anthropogenic seismicity is induced (though indirectly) by fluid injection (Bentz et al., 2020), this confirms that natural swarms are also a consequence of fluid pressure perturbations.

Second, the velocity-duration scaling is the same for swarms and for the SSEs reported by Gao et al. (2012), despite higher velocities for the latter, typically around 1 to 10 km/day. This confirms that the migration of swarms globally behaves as the propagation of aseismic slip, hence the assumption made of $V_{rupt} = V_{migr}$. The observed scaling for swarms, $\boldsymbol{V\alpha T^{-\gamma}}$ with $\boldsymbol{\gamma = 0.55}$, is compatible with fluid diffusion. However, a similar scaling is obtained for SSEs, which exhibit individual linear migrations (Houston et al., 2011) and are not driven by fluid diffusion. Other mechanisms have been proposed to explain such a scaling for SSEs, like a uniform stress drop or a uniform slip (Ide et al., 2007). These mechanisms might also be valid for swarms, explaining then the observed continuum of characteristics (Figure 2C). Therefore, a general scaling compatible with diffusion does not imply that individual swarm are directly driven by fluid diffusion.

The effective stress drop $\boldsymbol{\Delta\sigma_e}$ is found to range between 1 kPa and 1 MPa (Figure 3). Those values are lower than typical values of static stress drop for earthquakes, which usually range between 1 and 100 MPa (Cocco et al., 2016) and are more similar to the stress drop values of SSEs (Brodsky and Mori, 2007). Thus, they indicate an aseismic component in the swarm processes. For instance, $\boldsymbol{\Delta\sigma_e}$ =1kPa for the Soultz-sous-Forêt stimulation, indicates an important aseismic moment release, while $\boldsymbol{\Delta\sigma_e}$ = 1MPa for the Basel injection means that aseismic slip is relatively less important in this case. $\boldsymbol{\Delta\sigma_e}$ ranges in a similar way for natural and injection-induced sequences (Figure 3), indicating once again that mechanisms of seismic and aseismic moment release are controlled by the same processes for both types of sequences.

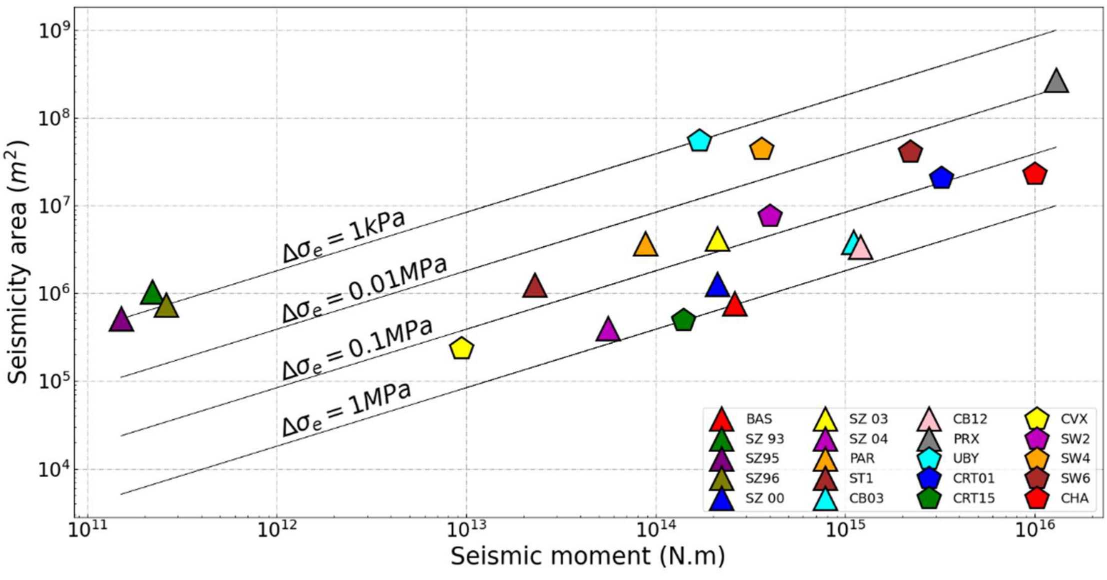

Figure 3. Seismicity area (m²) as a function of the cumulative seismic moment released during 20 of the swarms studied here. Triangles correspond to injection-induced sequences while pentagons refer to natural swarms. Black lines represent different values of the effective stress drop $\boldsymbol{\Delta\sigma_e}$.

Based on migration velocity and effective stress drop analysis, both natural and injection-induced swarms seem to share the same driving processes, in which aseismic slip seems ubiquitous, like depicted on Figure 1. The seismicity front is depicting the aseismic slip rupture propagation and the seismicity area corresponds to the aseismic slip area, in a similar way as tremors locations in SSEs zones delineate slip migration and area (Bartlow et al., 2011). However, the aseismic contribution might be different from one swarm to another.

3.2 Aseismic contribution differs among swarms

Once the total moment $\boldsymbol{M_{0,total}}$ for each swarm is computed, we compare it to the seismic moment released by using the seismic to total moment ratio *r* (Equation 7).

A value of *r* close to 1 indicates that moment release is mainly seismic, while a lower value shows that moment release is significantly aseismic. We compute $\boldsymbol{M_{0,total}}$ and *r* for the swarms studied here. As shown in Figure 4A, *r* ranges from 0.001 to almost 1. For the Basel injection-induced sequence, *r* = 0.97, suggesting that aseismic deformation is low in this case, while for the Ubaye natural swarm, r = 0.005, indicating an important aseismic moment release.

For the Soultz 1993 sequence, despite an injected fluid volume of the same order of magnitude as in the Basel injection (Diechmann et Giardini, 2009), the cumulative seismic moment is 3 orders of magnitude lower than the Basel one. This can be explained here by an important aseismic moment release (r ~ 0.001) taking place during the Soultz sequence. Therefore, the strong difference of seismic moment release for similar volumes can simply reflect the amount of induced aseismic deformation (McGarr and Barbour, 2018; De Barros et al., 2019).

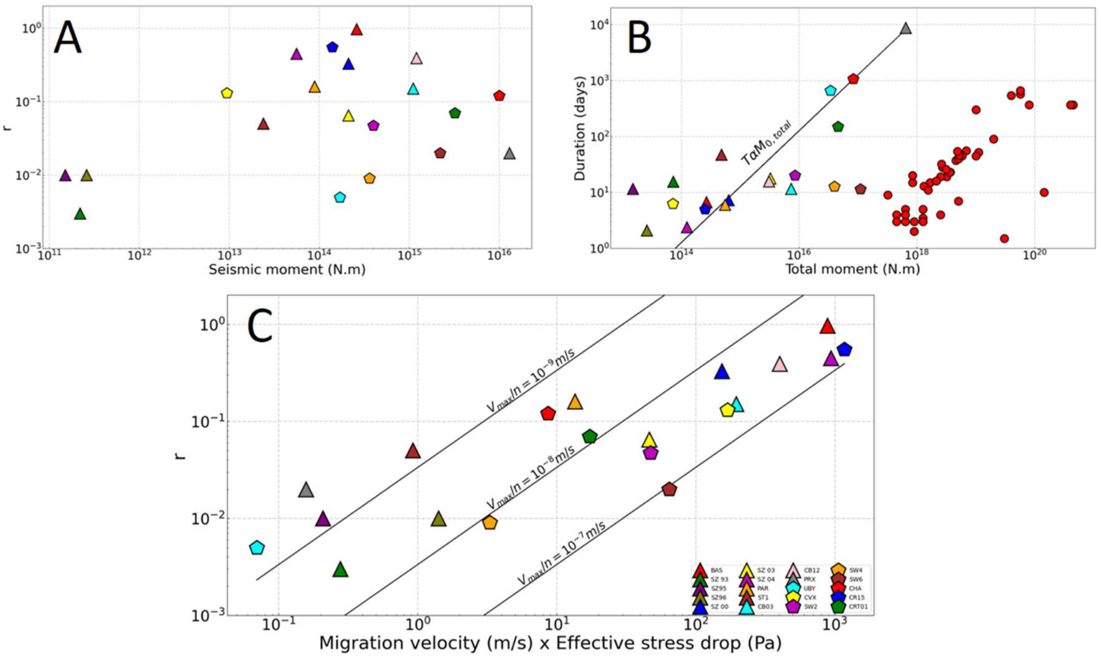

Figure 4. (**A**) Seismic to total moment ratio, as a function of the seismic moment released during each swarm, for the sequences studied here. (**B**) Duration as a function of the estimated total moment. Black line represents the 1:1 scaling. Red dots correspond to the SSE data from Gao et al., 2012. (**C**) Seismic to total moment ratio for the swarms studied here, as a function of the product of the migration velocity and the effective stress drop. The black lines correspond to different values of $\frac{V_{max}}{n}$, assuming G = 30GPa (see Equation 8).

Interestingly, one can also note that the scaling of duration with estimated total moment (Figure 4B) seems to be 1:1, similarly to the scaling between event duration and aseismic moment observed for SSEs (Ide et al., 2007; Peng and Gomberg, 2010), while seismic moment vs duration does not exhibit such a scaling (Passarelli et al., 2018). Indeed, with our total moment estimate, we are able to measure the “hidden” aseismic slip release. As hypothesized (Peng and Gomberg, 2010), the apparent branching off of the swarms in the moment duration can be corrected when considering the aseismic deformation.

Using Equation 8, we can relate the seismic to total moment ratio to two observables, effective stress drop and migration velocity (see Figure 4C). Following Equation 8, we estimate $\boldsymbol{V_{max}/n}$ being between $\mathbf{10^{-10}}$ and $\mathbf{10^{-7}}$ m/s, which is consistent with expected orders of magnitudes (Roland and McGuire, 2009; Glowacka et al., 2001) if we consider a value of n~10 (Hawthorne and Rubin, 2013; Lambert et al., 2021). Variability in $\boldsymbol{V_{max}}$ explains why the observed scaling between $\boldsymbol{r}$ and $\boldsymbol{\Delta\sigma_e * V_{migr}}$ is not as linear as expected. As the general trend shows a scaling different than the isovalues of V_{max}/n, it means that V_{max} also depends, through fault and stress properties, on the seismic-to-total seismic ratio. The slip velocity, together with the migration velocity and the effective stress drop, are the crucial parameters to characterize the seismic and aseismic moment partitioning in swarms. Among other properties, these three parameters depend on the stress state and on the proximity of the fault to failure (Hainzl and Fischer, 2002; Fischer and Hainzl, 2017; Passelègue et al., 2020; Wynants-Morel et al., 2020; De Barros et al., 2021). These relationships therefore deserve to be investigated in order to anticipate the swarm evolution, especially given that similarities are found between swarms and foreshock sequences of some major earthquakes (Chen and Shearer, 2013).

4. Conclusions

In this work, we confirmed that injection-induced and natural swarms are governed by the same physics, as was previously shown for particular sequences (Fischer and Hainzl, 2017). By analyzing sequences covering a wide range of geological contexts, migration velocities, durations and injected fluid volumes, we showed a global unity in the swarm's dynamics. After confirming that fluid-induced aseismic slip explains observations made on swarms, like their migration or their spatial seismic moment release, we exploited the similarities between swarms and slow slip events to introduce a simple mechanical framework that relates the seismic and aseismic moment partitioning to physical and observable parameters (Equation 8). This opens interesting perspectives to better understand swarms, their propagation, and improve their monitoring in order to anticipate potential large earthquakes. It also paves a way to studying natural and injection-induced swarms as the same phenomena.

Acknowledgments

Data for the Iceland swarms were kindly made available by the Icelandic Meteorological Office (SIL) and L. Passarelli (Passarelli et al., 2018). Data from the Paralana sequence and from the Ubaye swarm were made available by J. Albaric (Albaric et al., 2014*)* and G. Daniel (Daniel et al., 2011) respectively. Magnitudes for the Cahuilla swarm were provided by Z. Ross and D. Trugman (Ross et al., 2020). Data for the Soultz fluid injections are available on the CDGP web services. Data for the Cooper Basin injections are available on the EPOS platform. Data for the Paradox Valley fluid injection are available on the US Bureau of Reclamation.

References

Albaric, J., Oye, V., Langet, N., Hasting, M., Lecomte, I., Iranpour, K., ... & Reid, P. (2014). Monitoring of induced seismicity during the first geothermal reservoir stimulation at Paralana, Australia. *Geothermics*, *52*, 120-131.

Ampuero, J. P., & Rubin, A. M. (2008). Earthquake nucleation on rate and state faults–Aging and slip laws. *Journal of Geophysical Research: Solid Earth*, *113*(B1).

Baisch, S., Weidler, R., Vörös, R., Wyborn, D., & de Graaf, L. (2006). Induced seismicity during the stimulation of a geothermal HFR reservoir in the Cooper Basin, Australia. *Bulletin of the Seismological Society of America*, *96*(6), 2242-2256.

Baisch, S., Vörös, R., Weidler, R., & Wyborn, D. (2009). Investigation of fault mechanisms during geothermal reservoir stimulation experiments in the Cooper Basin, Australia. *Bulletin of the Seismological Society of America*, *99*(1), 148-158.

Baisch, Stefan and Rothert, Elmar and Stang, Henrik and Vörös, Robert and Koch, Christopher and McMahon, Andrew (2015) *Continued Geothermal Reservoir Stimulation Experiments in the Cooper Basin (Australia).* Bulletin of the Seismological Society of America, 105 (1). pp. 198-209

Bartlow, Noel M., et al. "Space-time correlation of slip and tremor during the 2009 Cascadia slow slip event." *Geophysical Research Letters* 38.18 (2011).

Bentz, S., Kwiatek, G., Martínez-Garzón, P., Bohnhoff, M., & Dresen, G. (2020). Seismic moment evolution during hydraulic stimulations. *Geophysical Research Letters*, *47*(5), e2019GL086185.

Bhattacharya, P., & Viesca, R. C. (2019). Fluid-induced aseismic fault slip outpaces pore-fluid migration. *Science*, *364*(6439), 464-468.

Bourouis, S., & Bernard, P. (2007). Evidence for coupled seismic and aseismic fault slip during water injection in the geothermal site of Soultz (France), and implications for seismogenic transients. *Geophysical Journal International*, *169*(2), 723-732.

Brodsky, E. E., & Mori, J. (2007). Creep events slip less than ordinary earthquakes. *Geophysical Research Letters*, *34*(16).

Calò, M., & Dorbath, C. (2013). Different behaviours of the seismic velocity field at Soultz-sous-Forêts revealed by 4-D seismic tomography: case study of GPK3 and GPK2 injection tests. *Geophysical Journal International*, *194*(2), 1119-1137.

Cappa, F., Scuderi, M. M., Collettini, C., Guglielmi, Y., & Avouac, J. P. (2019). Stabilization of fault slip by fluid injection in the laboratory and in situ, Sci.

Chen, T., & Lapusta, N. (2009). Scaling of small repeating earthquakes explained by interaction of seismic and aseismic slip in a rate and state fault model. *Journal of Geophysical Research: Solid Earth*, *114*(B1).

Chen, X., Shearer, P. M., & Abercrombie, R. E. (2012). Spatial migration of earthquakes within seismic clusters in Southern California: Evidence for fluid diffusion. *Journal of Geophysical Research: Solid Earth*, *117*(B4).

Chen, X., & Shearer, P. M. (2013). California foreshock sequences suggest aseismic triggering process. *Geophysical Research Letters*, *40*(11), 2602-2607.

Cocco, M., Tinti, E., & Cirella, A. (2016). On the scale dependence of earthquake stress drop. *Journal of Seismology*, *20*(4), 1151-1170.

Cuenot, N., Dorbath, C., & Dorbath, L. (2008). Analysis of the microseismicity induced by fluid injections at the EGS site of Soultz-sous-Forêts (Alsace, France): implications for the characterization of the geothermal reservoir properties. *Pure and Applied Geophysics*, *165*(5), 797-828.

Daniel, G., et al. (2011), Changes in effective stress during the 2003–2004 Ubaye seismic swarm, France, *J. Geophys. Res.*, 116, B01309

De Barros, L. ,Guglielmi, Y., Rivet, D., Cappa, F., Duboeuf, L. (2018). Comptes Rendus Geoscience 350, 464 Invited contributions by 2016–2017 geoscience laureates of the French Academy of Sciences.

De Barros, L., Baques, M., Godano, M., Helmstetter, A., Deschamps, A., Larroque, C., & Courboulex, F. (2019). Fluid-induced swarms and coseismic stress transfer: A dual process highlighted in the aftershock sequence of the 7 April 2014 earthquake (Ml 4.8, Ubaye, France). *Journal of Geophysical Research: Solid Earth*, 124, 3918– 3932.

De Barros, L., Cappa, F., Guglielmi, Y., Duboeuf, L., & Grasso, J. R. (2019). Energy of injection-induced seismicity predicted from in-situ experiments. *Scientific reports*, *9*(1), 1-11.

De Barros, L., Cappa, F., Deschamps, A., & Dublanchet, P. (2020). Imbricated aseismic slip and fluid diffusion drive a seismic swarm in the Corinth Gulf, Greece. *Geophysical Research Letters*, *47*(9), e2020GL087142.

De Barros, L., Wynants-Morel, N., Cappa, F., & Danré, P. (2021). Migration of fluid-induced seismicity reveals the seismogenic state of faults. *Journal of Geophysical Research: Solid Earth*, 126, e2021JB022767.

Deichmann, N., & Giardini, D. (2009). Earthquakes induced by the stimulation of an enhanced geothermal system below Basel (Switzerland). *Seismological Research Letters*, *80*(5), 784-798.

Duboeuf, L. (2018). *Injections de fluide dans une zone de faille (LSBB, Rustrel): sismicité induite et déformation asismique* (Doctoral dissertation, Université Côte d'Azur).

Duverger, C., Godano, M., Bernard, P., Lyon-Caen, H., & Lambotte, S. (2015). The 2003–2004 seismic swarm in the western Corinth rift: Evidence for a multiscale pore pressure diffusion process along a permeable fault system. *Geophysical Research Letters*, *42*(18), 7374-7382.

Duverger, C., Lambotte, S., Bernard, P., Lyon-Caen, H., Deschamps, A., & Nercessian, A. (2018). Dynamics of microseismicity and its relationship with the active structures in the western Corinth Rift (Greece). *Geophysical Journal International*, *215*(1), 196-221.

Dyer, B., R. Baria, et S. Michelet. 2004. « Soultz GPK3 stimulation and GPK3-GPK2 circulation May to July 2003 - Seismic monitoring report ». Report n° EEIG 05/2004. Semore Seismic for Socomine.

Edwards, B., & Douglas, J. (2014). Magnitude scaling of induced earthquakes. *Geothermics*, *52*, 132-139.

Fischer, T., & Hainzl, S. (2017). Effective stress drop of earthquake clusters. *Bulletin of the Seismological Society of America*, *107*(5), 2247-2257.

Fischer, T., & Hainzl, S. (2021). The growth of earthquake clusters. *Frontiers in Earth Science*, *9*, 79.

Gao, H., Schmidt, D. A., & Weldon, R. J. (2012). Scaling relationships of source parameters for slow slip events. *Bulletin of the Seismological Society of America*, *102*(1), 352-360.

Gerard, A., Baumgärtner, J., Baria, R., & Jung, R. (1997). An attempt towards a conceptual model derived from 1993−1996 hydraulic operations at Soultz. In Proceedings of NEDO International Symposium, Sendai, Japan (Vol. 2, pp. 329–341).

Glowacka, E., González, J. J., Nava, F. A., Farfan, F., & Diaz de Cossio, G., Monitoring surface deformations in the Mexicali valley, BC, Mexico Proceedings of tenth international symposium on deformation measurements (Vol. 175183) (2001)

Goebel, T. H., & Brodsky, E. E. (2018). The spatial footprint of injection wells in a global compilation of induced earthquake sequences. *Science*, *361*(6405), 899-904.

Goertz-Allmann, B. P., Goertz, A., and Wiemer, S. (2011), Stress drop variations of induced earthquakes at the Basel geothermal site, *Geophys. Res. Lett.*, 38, L09308,

Gualandi, A., Nichele, C., Serpelloni, E., Chiaraluce, L., Anderlini, L., Latorre, D., ... & Avouac, J. P. (2017). Aseismic deformation associated with an earthquake swarm in the northern Apennines (Italy). *Geophysical Research Letters*, *44*(15), 7706-7714.

Guglielmi, Y., Cappa, F., Avouac, J. P., Henry, P., & Elsworth, D. (2015). Seismicity triggered by fluid injection–induced aseismic slip. *Science*, *348*(6240), 1224-1226.

Hainzl, S., & Fischer, T. (2002). Indications for a successively triggered rupture growth underlying the 2000 earthquake swarm in Vogtland/NW Bohemia. *Journal of Geophysical Research: Solid Earth*, *107*(B12), ESE-5.

Hawthorne, J. C., & Rubin, A. M. (2013). Laterally propagating slow slip events in a rate and state friction model with a velocity-weakening to velocity-strengthening transition. *Journal of Geophysical Research: Solid Earth*, *118*(7), 3785-3808.

Hawthorne, J. C., Ampuero, J. P., & Simons, M. (2017). A method for calibration of the local magnitude scale based on relative spectral amplitudes, and application to the San Juan Bautista, California, area. *Bulletin of the Seismological Society of America*, *107*(1), 85-96.

Herrmann, M., Kraft, T., Tormann, T., Scarabello, L., & Wiemer, S. (2019). A consistent high-resolution catalog of induced seismicity in Basel based on matched filter detection and tailored post-processing. *Journal of Geophysical Research: Solid Earth*, *124*(8), 8449-8477.

Hincks, T., Aspinall, W., Cooke, R., & Gernon, T. (2018). Oklahoma's induced seismicity strongly linked to wastewater injection depth. *Science*, *359*(6381), 1251-1255.

Hong, T. K., Park, S., Lee, J., Chung, D., & Kim, W. (2020). One-off deep crustal earthquake swarm in a stable intracontinental region of the southwestern Korean Peninsula. *Physics of the Earth and Planetary Interiors*, *308*, 106582.

Houston, H., Delbridge, B. G., Wech, A. G., & Creager, K. C. (2011). Rapid tremor reversals in Cascadia generated by a weakened plate interface. *Nature Geoscience*, *4*(6), 404-409.

Ide, S., Beroza, G. C., Shelly, D. R., & Uchide, T. (2007). A scaling law for slow earthquakes. *Nature*, *447*(7140), 76-79.

Ito, Y., Obara, K., Shiomi, K., Sekine, S., & Hirose, H. (2007). Slow earthquakes coincident with episodic tremors and slow slip events. *Science*, *315*(5811), 503-506.

Jenatton, L., Guiguet, R., Thouvenot, F., & Daix, N. (2007). The 16,000-event 2003–2004 earthquake swarm in Ubaye (French Alps). *Journal of Geophysical Research: Solid Earth*, *112*(B11).

Kim, W. Y. (2013). Induced seismicity associated with fluid injection into a deep well in Youngstown, Ohio. *Journal of Geophysical Research: Solid Earth*, *118*(7), 3506-3518.

Kwiatek, G., Saarno, T., Ader, T., Bluemle, F., Bohnhoff, M., Chendorain, M., ... & Wollin, C. (2019). Controlling fluid-induced seismicity during a 6.1-km-deep geothermal stimulation in Finland. *Science advances*, *5*(5), eaav7224.

Lambert, V., Lapusta, N., & Faulkner, D. (2021). Scale dependence of earthquake rupture prestress in models with enhanced weakening: implications for event statistics and inferences of fault stress. *Earth and Space Science Open Archive*, 55.

Larochelle, S., Lapusta, N., Ampuero, J. P., & Cappa, F. (2021). Constraining Fault Friction and Stability With Fluid-Injection Field Experiments. *Geophysical Research Letters*, e2020GL091188.

Lengliné, O., Lamourette, L., Vivin, L., Cuenot, N., & Schmittbuhl, J. (2014). Fluid-induced earthquakes with variable stress drop. *Journal of Geophysical Research: Solid Earth*, *119*(12), 8900-8913.

Lengliné, O., Boubacar, M., & Schmittbuhl, J. (2017). Seismicity related to the hydraulic stimulation of GRT1, Rittershoffen, France. *Geophysical Journal International*, *208*(3), 1704-1715

Lohman, R. B., & McGuire, J. J. (2007). Earthquake swarms driven by aseismic creep in the Salton Trough, California. *Journal of Geophysical Research: Solid Earth*, *112*(B4).

Madariaga, R. Dynamics of an expanding circular fault. *Bulletin of the Seismological Society of America*, *66*(3), 639-666.(1976)

Matsuzawa, T., Uchida, N., Igarashi, T., Okada, T., & Hasegawa, A. (2004). Repeating earthquakes and quasi-static slip on the plate boundary east off northern Honshu, Japan. *Earth, planets and space*, *56*(8), 803-811.

McGarr, A., & Barbour, A. J. (2018). Injection-induced moment release can also be aseismic. *Geophysical Research Letters*, *45*(11), 5344-5351.

Passarelli, L., Rivalta, E., Jónsson, S., Hensch, M., Metzger, S., Jakobsdóttir, S. S., ... & Dahm, T. (2018). Scaling and spatial complementarity of tectonic earthquake swarms. *Earth and Planetary Science Letters*, *482*, 62-70.

Passelègue, F. X., Almakari, M., Dublanchet, P., Barras, F., Fortin, J., & Violay, M. (2020). Initial effective stress controls the nature of earthquakes. *Nature communications*, *11*(1), 1-8.

Peng, Z., & Gomberg, J. (2010). An integrated perspective of the continuum between earthquakes and slow-slip phenomena. *Nature geoscience*, *3*(9), 599-607.

Roland, E., & McGuire, J. J. (2009). Earthquake swarms on transform faults. *Geophysical Journal International*, *178*(3), 1677-1690.

Ross, Z. E., Cochran, E. S., Trugman, D. T., & Smith, J. D. 3D fault architecture controls the dynamism of earthquake swarms. *Science*, *368*(6497), 1357-1361. (2020)

Rubin, A. M. (2008). Episodic slow slip events and rate-and-state friction. *Journal of Geophysical Research: Solid Earth*, *113*(B11).

Schmidt, D. A., & Gao, H. (2010). Source parameters and time-dependent slip distributions of slow slip events on the Cascadia subduction zone from 1998 to 2008. *Journal of Geophysical Research: Solid Earth*, *115*(B4).

Seeber, L., Armbruster, J. G., & Kim, W. Y. (2004). A fluid-injection-triggered earthquake sequence in Ashtabula, Ohio: Implications for seismogenesis in stable continental regions. *Bulletin of the Seismological Society of America*, *94*(1), 76-87.

Shapiro, S. A., Huenges, E., & Borm, G. (1997). Estimating the crust permeability from fluid-injection-induced seismic emission at the KTB site. *Geophysical Journal International*, *131*(2), F15-F18.

Uchida, N. (2019). Detection of repeating earthquakes and their application in characterizing slow fault slip. *Progress in Earth and Planetary Science*, *6*(1), 1-21.

Wei, et al., The 2012 Brawley swarm triggered by injection-induced aseismic slip Earth and Planetary Science Letters 422, 115 (2015).

Wynants-Morel, N., Cappa, F., De Barros, L., & Ampuero, J. P. (2020). Stress perturbation from aseismic slip drives the seismic front during fluid injection in a permeable fault. *Journal of Geophysical Research: Solid Earth*, *125*(7), e2019JB019179.

Yeck, W. L., Block, L. V., Wood, C. K., & King, V. M. (2015). Maximum magnitude estimations of induced earthquakes at Paradox Valley, Colorado, from cumulative injection volume and geometry of seismicity clusters. *Geophysical Journal International*, *200*(1), 322-336.